International Journal of Engineering

Journal Homepage: www.ije.ir

Application of Ultra-sensitive Pillar-enhanced Quartz Crystal Resonators for Airborne Detection of Nanoparticles: A Theoretical Study

X. Xie*[a], B. Zheng[b]

[a] *Nanjing University, Gulou, Nanjing, Jiangsu, China*
[b] *Lanzhou University, Lanzhou, Gansu, China*

PAPER INFO

Paper history:
Received 04 April 2023
Received in revised form 25 April 2023
Accepted 26 April 2023

Keywords:
Quartz Crystal Resonator
Micropillar
Nanoparticle
Bandwidth
Ultra-sensitive Actuator

ABSTRACT

Although quartz crystal resonators (QCR) have been used for airborne detection of particles and viruses, they suffer from various limitations, such as low sensitivity compared to other devices. Therefore, it is necessary to develop a new device capable of achieving high sensitivity, which can be used for practical airborne detections. The current study reports a comprehensive parametric theoretical model for analyzing the response of ultra-sensitive pillar-enhanced QCR (QCR-P) for airborne detection of nanoparticles. The electromechanical model comprised an equivalent circuit integrated with pillars containing nanoparticles. It was shown that pillar height and particle radius play a critical role in the response of QCR-P devices. The study revealed that selecting the optimal pillar height can lead to a significant frequency shift depending on the nanoparticle radius and pillar height, while it is independent of particle mass density. These results underscore the potential of utilizing pillars to substantially enhance the sensitivity of conventional QCR up to 140 times in the airborne detection of nanoparticles. These findings can be utilized to design optimum pillar heights to achieve maximum sensitivity in the airborne detection of nanoparticles and proteins, thereby enabling the adoption of ultra-sensitive pillar-enhanced quartz crystal resonators for practical airborne applications.

doi: *10.5829/ije.2023.36.06c.12*

1. INTRODUCTION

Detection of proteins and nanoparticles has gained increasing attention in various applications, such as immunosensors and breath analyzers [1, 2]. For indication, Farsaeivahid et al. [3] developed an electrochemical device to detect the COVID-19 virus. In another study, they utilized X-Fe_2O_4-buckypaper nanocomposites for nonenzymatic electrochemical glucose biosensing [4, 5]. Compared to other devices, AT-cut quartz crystal resonator (QCR) devices have shown great potential as airborne detecting sensors [6]. The adhered mass on the QCR substrate can be calculated by using the observed frequency of the QCR in the Sauerbrey theory [7]. Generally, a thin film of polymer or fiber [8] is fabricated on the substrate, enabling the device to detection of particles, organic compounds, bacteria, colloidal particles, and cells [9, 10]. Pato et al. [11] analyzed the physicochemical properties of cellulose in order to evaluate the efficacy of the hydrogel. Budianto et al. [12] developed a QCR coated with graphene oxide for measuring fungal spore mass. The developed system exhibited strong performance with sensitivities ranging from 27×10^{-2} to 29×10^{-2} Hz/ng. In another study, Lee et al. [13] aimed at airborne detection of vaccinia viruses using highly sensitive QCR. They concluded that the QCR has great potential for the quantitative detection of airborne viruses. QCR devices coated with monoclonal antibodies have also been utilized as immunosensor for airborne cat allergens [14]. It was shown that the QCR is capable of achieving a low limit of detection due to high sensitivity and selectivity. Although QCR-based devices have been used for airborne detection of particles and viruses, they suffer from various limitations, such as low sensitivity compared to other immunosensors. Therefore, it is necessary to develop a new device capable of achieving high sensitivity, which can be used for real-time airborne detections.

*Corresponding Author Email: xuanxie263@gmail.com (X. Xie)

Please cite this article as: X. Xie, B. Zheng, Application of Ultra-sensitive Pillar-enhanced Quartz Crystal Resonators for Airborne Detection of Nanoparticles: A Theoretical Study, ***International Journal of Engineering, Transactions C: Aspects***, Vol. 36, No. 06, (2023), 1136-1142

Microbeams have recently been printed on QCR surfaces to characterize their geometric/physical features and develop a coupled sensor [15, 16]. As the pillar height approaches critical values, the frequency jump is generated by resonance between the pillars and QCR [17]. By selecting proper pillar characteristics, such as height, one can increase mass sensitivity by lowering the frequency shift produced by even a nanoscale change in the size of the pillars at this moment [18]. For single monolayer films, the mass sensitivity and reaction time of coupled sensors were also studied [19]. The effect of the contact area of the SU-8 pillar on the QCR was studied by Kashan et al. [20].

Numerical and analytical models have been widely used to analyze the fundamental behavior of mechanical systems [21-23]. For example, Abdollahi et al. [24] developed a finite element model (FEM) to analyze the impact of hybrid nanofluid on the flow field and heat transfer in parallel surfaces. In the case of coupled QCR-pillar devices, numerical models have been widely applied. Kashan et al. [25] developed a finite element model (FEM) to analyze the resonance frequency of coupled QCR-pillars (QCR-P). Wang et al. [26] utilized coupled QCR with polymer pillars to numerically analyze the liquid penetration from the Cassie state to the Wenzel state. Esfahani and Sun [27] developed a droplet-based QCR-P device to study the viscosity of sample solutions. Liquid loading on the QCR was calculated using COMSOL simulation, and Kerr-lens mode-locked (KLM) equivalent circuit was used to calculate the resonance frequency of QCR. They observed that the QCR-micropillar can produce up to 20 times sensitivity enhancement compared to conventional QCR devices [27]. While these studies are largely concerned with surface wetting and viscosity measurements, they do not address the impact of solid particle detection, such as colloidal particles and bacteria on the response of coupled QCR-P devices.

Despite extensive research into the influence of pillars on the resonance frequency of QCR, there is a significant research gap pertaining to the application of QCR-P devices for the airborne detection of particles. The use of QCR-P devices has the potential to enhance the sensitivity of conventional QCR devices in detecting airborne particles in real time, thereby enabling their widespread adoption in real-world applications. In view of this, it becomes imperative to undertake an in-depth study of the response of QCR-P devices containing nanoparticles. The current investigation presents a groundbreaking electromechanical model that facilitates the analysis of the response of QCR-P devices with adhered nanoparticles on the tip of the pillars. Specifically, this study explores the correlation between the response of the QCR-P device and the characteristics of adherent nanoparticles, thereby providing invaluable insights into the design of optimum pillars to achieve maximum sensitivity in detecting nanoparticles. The findings of this study have significant implications for future research on the development and optimization of QCR-P devices for diverse airborne applications.

In section 2, we discussed the methodology for the analytical model. In section 3, we presented the result in detail and discussed the key points of QCR-P for airborne detection of nanoparticles. A comparison of our model with existing experimental measurements is also shown in section 3. Finally, in section 4, the results are analyzed, and the conclusions are made for this study.

2. THEORETICAL ANALYSIS

2. 1. Load Impedance Calculation It is assumed that the main displacement of pillars is in the y-direction, and the displacement in other directions is negligible. Also, pillars have the same characteristics and vibrational states for simplicity of the calculations. The equation of pillar motion for an element with a thickness of *dz* is shown in Figure 1(a) [28]:

$$F + \frac{\partial F}{\partial z} dz - F = (\rho A dz) \frac{\partial^2 u}{\partial t^2} \quad (1)$$

where u is the displacement, A is the cross-sectional area, ρ is the density, and t is the time. The shear force (F) can be calculated as:

$$F = \kappa A G \frac{\partial u}{\partial z} \quad (2)$$

where G is the complex shear modulus, and κ is the shear coefficient of pillars. Using Equation (2) in Equation (1), the equation of pillar motion can be represented as follows:

$$\frac{\partial^2 u}{\partial z^2} + \lambda^2 u = 0 \quad (3)$$

where:

$$\lambda^2 = \frac{\omega^2 \rho}{\kappa G} \quad (4)$$

It is assumed that the nanoparticles are rigidly attached to the tip of pillars. A shear force is applied to the top surface of pillars due to the vibration of nanoparticles which is represented in Figure 1(b):

$$F(H) = -m_p \omega^2 u(H) \quad (5)$$

where H is the height of the pillar, m_p is the mass of an attached particle, and ω is the angular frequency. The displacement at the bottom of the pillars can be represented as:

$$u(0) = u_0 \quad (6)$$

where u_0 is the displacement of the top surface of QCR. Using boundary conditions (Equations (5) and (6)) in Equation (3), the displacement of pillars with rigidly attached nanoparticles can be calculated as:

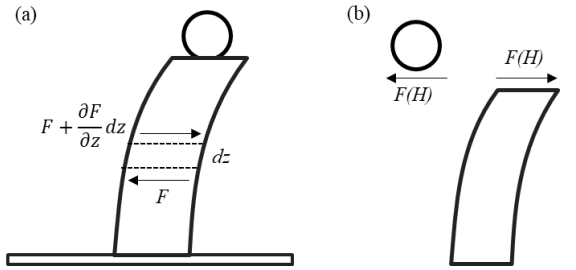

Figure 1. (a) shear vibration of a pillar in air medium (b) shear force acting on the pillar-particle interface

$$u = C_1 \cos \lambda z + C_2 \sin \lambda z \quad (7)$$

where:

$$C_1 = u_0 \quad (8)$$

$$C_2 = \frac{\kappa AG\lambda \sin \lambda H - m_p \omega^2 \cos \lambda H}{\kappa AG\lambda \cos \lambda H + m_p \omega^2 \sin \lambda H} u_0 \quad (9)$$

Based on Equation (7), the load impedance (Z_L) applied to a top surface of QCR can be evaluated as [28]:

$$Z_L = -\frac{\kappa AG\lambda C_2}{i\omega u_0} \quad (10)$$

2. 2. QCR-pillar Coupling In the current study, it is assumed that the obtained shift is significantly lower compared to the quartz resonance frequency. Thus, a small load approximation technique is used to couple the QCR resonator with pillars [29, 30]. The response of QCR with load impedance on the surface can be calculated as:

$$\frac{\Delta f + i\Delta \Gamma}{f_0} = \frac{iZ_L}{\pi Z_q} \quad (11)$$

where Δf is the frequency shift, $\Delta\Gamma$is the bandwidth shift, f_0 is the quartz resonance frequency, and Z_q is the quartz characteristic impedance. According to Equation (11), the frequency shift and bandwidth shift of coupled QCR-pillar can be evaluated as:

$$\frac{\Delta f}{f_0} = Re\left(\frac{iZ_L}{\pi Z_q}\right) \quad (12)$$

$$\frac{\Delta \Gamma}{f_0} = Im\left(\frac{iZ_L}{\pi Z_q}\right) \quad (13)$$

For theoretical example, we considered 10 MHz AT-cut quartz resonators with f_0 = 10 MHz and $Z_q = 8.8 \times 10^6$ $kgm^{-2}s^{-1}$. The materials of pillars are SU-8 with a shear modulus of $G = 1.66 \times 10^9 + 1i\ (6 \times 10^7)$, a density of ρ = 1200 kgm^{-3}, a cross-sectional radius of R = 0.25 μm, and a shear coefficient of κ = 0.9. Figure 2 summarizes the flow chart of the developed methodology for predicting the response of QCR carrying an array of pillars with nanoparticles.

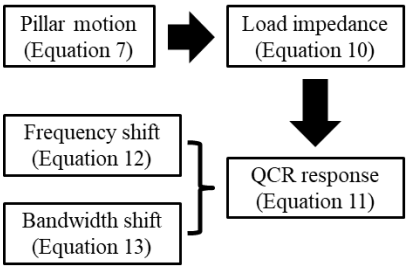

Figure 2. Flow chart of the developed model

3. RESULTS AND DISCUSSION

3. 1. Special Case: No Particles In order to validate the model, we consider a special case where no particles are attached to the pillars. In this case, it is assumed that the attached particles have a mass of m_p = 0. The model prediction was compared with the previous experimental measurement using PMMA pillars in the air [27]. It should be noted that the size and detail of the pillars can be found in literature [27].The results are shown in Figure 3. The prediction of the model is in good agreement with experimental measurements. As the height increased, the frequency of the QCR-P decreased. When the pillar height approached a specific height, known as "resonance height", a sudden drop-jump was observed in the response of the device. This is related to the elastic loading of the pillar on the QCR substrate. When the height is much smaller than the resonance height, the pillar acts as inertial loading on the QCR substrate, consistent with the Saurebrey theory. However, the pillar coupled with QCR acts as an elastic loading on the QCR substrate at the resonance height, resulting in a phase-veering behavior in the pillar vibration. When the pillar is smaller than the resonance height, the pillar's displacements are in the same phase as the QCR. A phase shift occurs when the pillar is larger

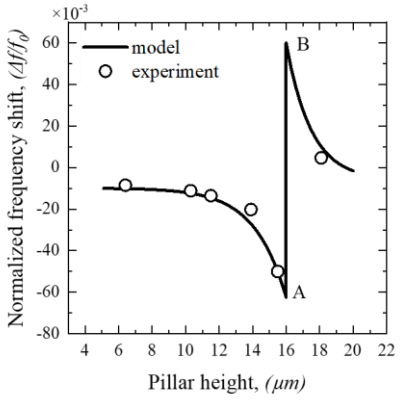

Figure 3. Model prediction of the frequency shift of QCR-P at various pillar heights vs. experimental measurements [27]

than the resonance height, leading to the out-phase vibration of pillars and QCR. This phase-veering phenomenon results in a sudden drop-and-jump in the device's response. It is believed that the discrepancies between the experimental measurements and the model are due to the thickness of the residual layer in experimental measurements.

The sensitivity of the QCR-P with respect to pillar height is shown in Figure 4. It should be noted that the sensitivity of QCR-P is normalized with respect to the sensitivity of conventional QCR. As can be seen, the sensitivity of the QCR-P is close to conventional QCR when the pillar height is small. As the pillar height increases, the sensitivity of the QCR-P increases. The maximum sensitivity is achieved at the resonance height, which is consistent with previous experimental measurements. It is also noticed that a small shift in the height of the QCR-P can result in a significant shift in the sensitivity of the device when the pillar height is at resonance height. Therefore, it is necessary to consider the accuracy of the fabrication procedure of pillars on the QCR when the height is close to the resonance point.

Figure 5 shows the displacement of pillars in points A and B. As can be seen, a phase shift is observed in the displacements. Pillars vibrate in phase with the QCR when the height is lower than the resonance height, resulting in inertial loading on the device. However, an out-phase vibration of pillars is obtained when the height is higher than the resonance height, indicating elastic loading on the device.

3. 2. Impact of Adhered Particles on Microbeams

To rigorously study the response of coupled QCR-pillar, it is necessary to model the impact of nanoparticles on the QCR-P. Figure 6(a) represents the effect of particle radius with a density of 1200 kg/m^3 on the resonance frequency shift of QCR-P devices. The behavior of QCR-P can be divided into two categories: below resonance height (A), and above resonance height (B). When the height is lower than resonance height (A), as the radius increases, a positive frequency shift is obtained, which is inconsistent with the Sauerbrey theory. This is related to the couple resonance phenomena between pillars and QCR. With an increase in the radius, the hydrodynamic loading on the tip of the pillar increases, resulting in decreasing the equivalent height of the QCR-P device. However, a different trend is observed when the pillar height is higher than the resonance height (B). In these cases, as the radius increases, the frequency shift increases. A sudden jump and drop behavior is observed at the critical particle radius due to decreasing the equivalent pillar height. Figure 6(b) indicates the effect of particle radius with a density of 1200 kg/m^3 on the bandwidth shift of QCR-P devices. The QCR-P behavior is consistent with the resonance frequency shift and the equivalent height analysis. When the height of the pillar is above resonance height (B), as the radius increases, the bandwidth increases. It reaches its maximum at the critical radius and decreases afterward. However, when the pillar height is lower than the resonance height, a constant decrease in the bandwidth is observed.

Figure 7 represents the sensitivity enhancement of QCR-P devices for airborne detection of nanoparticles compared to conventional QCR-based devices. It should be noted that the sensitivity of QCR-P was normalized to that of a conventional QCR device. As can be seen, as the

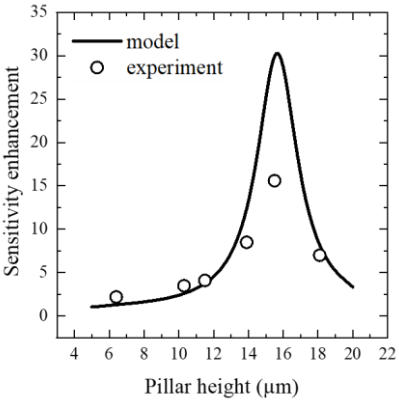

Figure 4. Model prediction of the sensitivity of QCR-P with respect to pillar height vs. experimental measurements [27]

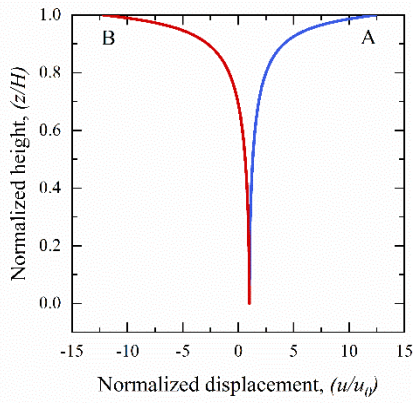

Figure 5. Displacement of pillars at points A and B

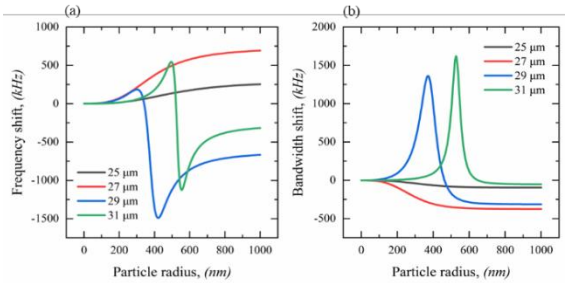

Figure 6. Frequency shift (a) and bandwidth shift (b) of QCR-P with nanoparticles with respect to particle radius

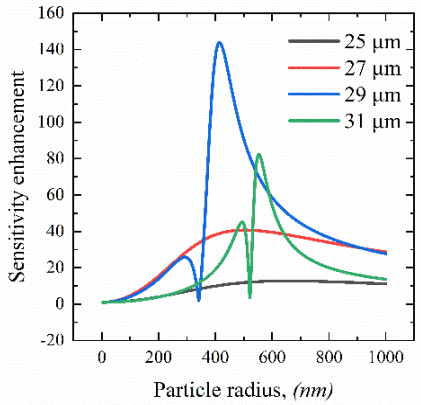

Figure 7. Sensitivity enhancement of QCR-P with respect to particle radius at different pillar heights

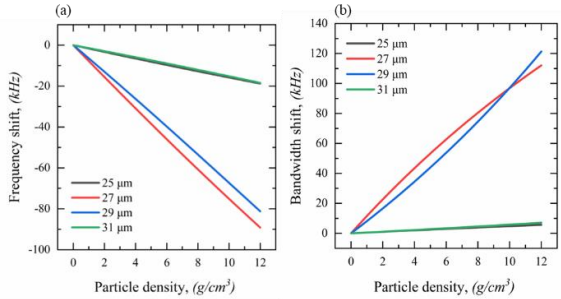

Figure 8. Frequency shift (a) and bandwidth shift (b) of QCR-P with nanoparticle with respect to particle radius

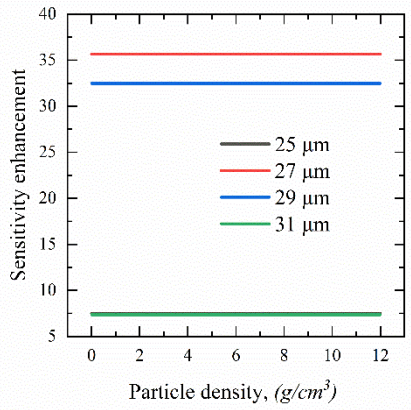

Figure 9. Sensitivity enhancement of QCR-P with respect to particle density at various pillar heights

particle radius increases, the sensitivity of QCR-P devices increases. For pillar height lower than resonance height, the sensitivity enhancement of QCR-P devices tends to become stable at higher radiuses of nanoparticles. However, the QCR-P devices with pillar height higher than resonance height follow a different trend. In these cases, the sensitivity enhancement increases as the particle radius increases. Then, it starts to decrease and suddenly increases until reaching maximum enhancement. With a further increase in particle radius, the sensitivity enhancement decreases. These results highlight that the pillar height higher than the resonance height has superior performance compared to pillar heights lower than the resonance height. Furthermore, QCR-P devices have the potential to achieve 140-times sensitivity enhancement for airborne detection of nanoparticles compared to conventional QCR, which makes them a suitable candidate for the practical application of QCR-P devices.

Figure 8 represents the effect of particle density with a radius of 100 nm on the resonance frequency and bandwidth shifts of QCR-P devices. Except for no jump existing because of no resonance, similar trends, and characteristics can be found in these two figures. As the density increases, the mass on the device increases, resulting in a negative frequency shift and positive bandwidth shift of QCR-P devices.

At last, the effect of particle density on the sensitivity of QCR-P devices is plotted in Figure 9. As can [be] seen, with increasing particle density, the sensitivity of QCR-P devices remains unchanged, indicating that the density of the particle has a negligible impact on the sensitivity. In addition, the results indicated that the micropillars near the resonance height show higher sensitivity than others. For indication, the pillars with a height of 25 µm have a sensitivity enhancement of 7.4, while it increases substantially to 35.6 as the pillar height approaches 27 µm.

4. CONCLUSION

In this study, the application of ultra-sensitive pillar-enhanced quartz crystal resonator (QCR-P) devices for the airborne detection of nanoparticles was theoretically investigated. An analytical model was developed by calculating the induced load impedance on the QCR substrate due to the array of pillars carrying nanoparticles on the tip. Then, a small load approximation technique was applied to predict the frequency and bandwidth shifts of the QCR. The developed model was validated by comparing the prediction results with previous experimental measurements for QCR-P in air. The study revealed that the sensitivity enhancement of QCR-P devices significantly depends on the particle radius and the pillar height, while it is independent of the particle mass density. It was obtained that selecting the optimal pillar height can substantially enhance the sensitivity of conventional QCR up to 140 times for the airborne detection of nanoparticles. Furthermore, we observed that as the pillar height approaches the resonance height, the sensitivity of QCR-P increases, indicating that fabricating pillars close to resonance height can lead to ultra-sensitivity of the device. The obtained results can help the researchers in designing optimum pillar height

in order to achieve maximum sensitivity for airborne detection of the nanoparticles, paving the way for adopting pillar-enhanced quartz crystal resonators for real-world applications such as breath analyzers. For future work, an experimental setup for measuring the response of QCR-P for airborne detection of nanoparticles or proteins will be initiated, with the goal of achieving ultra-high sensitive QCR by fabricating pillars at optimum pillar height.

5. REFERENCES

1. Kadam, V., Deshmukh, A. and Bhosale, S., "Hybrid beamforming for dual functioning multi-input multi-output radar using dimension reduced-baseband piecewise successive approximation", ***International Journal of Engineering***, ***Transactions A: Basics,*** Vol. 36, No. 1, (2023), 182-190. doi: 10.5829/IJE.2023.36.01A.20.
2. Nistratov, A.V., Klimenko, N.N., Pustynnikov, I.V. and Vu, L.K., "Thermal regeneration and reuse of carbon and glass fibers from waste composites", ***Emerging Science Journal***, Vol. 6, (2022), 967-984. doi: 10.28991/ESJ-2022-06-05-04.
3. Farsaeivahid, N., Grenier, C., Nazarian, S. and Wang, M.L., "A rapid label-free disposable electrochemical salivary point-of-care sensor for sars-cov-2 detection and quantification", ***Sensors***, Vol. 23, No. 1, (2022), 433. doi: 10.3390/s23010433.
4. Vahid, N.F., Marvi, M.R., Naimi-Jamal, M.R., Naghib, S.M. and Ghaffarinejad, A., "X-fe2o4-buckypaper-chitosan nanocomposites for nonenzymatic electrochemical glucose biosensing", ***Anal. Bioanal. Electrochem***, Vol. 11, No., (2019), 930-942.
5. Farsaei Vahid, N., Marvi, M.R., Naimi-Jamal, M.R., Naghib, S.M. and Ghaffarinejad, A., "Effect of surfactant type on buckypaper electrochemical performance", ***Micro & Nano Letters***, Vol. 13, No. 7, (2018), 927-930. doi: 10.1049/mnl.2017.0691.
6. Ji, S., Chiniforooshan Esfahani, I., Sun, H. and Wan, K.-t., "Particle deposition on a filtration bed using a quartz crystal microbalance embedded in a microfluidic channel", ***SSRN Electronic Journal***, doi: 10.2139/ssrn.4265353.
7. Ji, S., Ran, R., Chiniforooshan Esfahani, I., Wan, K.-t. and Sun, H., "A new microfluidic device integrated with quartz crystal microbalance to measure colloidal particle adhesion", in ASME International Mechanical Engineering Congress and Exposition, American Society of Mechanical Engineers. Vol. 85598, (2021), V005T005A075.
8. Hashim, A.M. and Kadhum, M.M., "Compressive strength and elastic modulus of slurry infiltrated fiber concrete (SIFCON) at high temperature", ***Civil Engineering Journal***, Vol. 6, No. 2, (2020), 265-275. doi: 10.28991/cej-2020-03091469.
9. Marchione, F., "Investigation of vibration modes of double-lap adhesive joints: Effect of slot", ***International Journal of Engineering, Transactions A: Basics,*** Vol. 33, No. 10, (2020), 1917-1923. doi: 10.5829/ije.2020.33.10a.10.
10. Karevan, M., Motalleb, M., Jannesari, A. and Zeinali, M., "High energy release-high retraction smart polymer fibers used in artificial muscle fabrication", ***International Journal of Engineering***, ***Engineering, Transactions A: Basics***, Vol. 36, No. 4, (2023), 788-796. doi: 10.5829/IJE.2023.34.04A.15
11. Pato, U., Ayu, D.F., Riftyan, E., Restuhadi, F., Pawenang, W.T., Firdaus, R., Rahma, A. and Jaswir, I., "Cellulose microfiber encapsulated probiotic: Viability, acid and bile tolerance during storage at different temperature", ***Emerging Science Journal***, Vol. 6, (2022), 106-117. doi: 10.28991/ESJ-2022-06-01-08.
12. Budianto, A., Wardoyo, A.Y.P., Masruroh, H.A.D. and Dharmawan, H., "An airborne fungal spore mass measurement system based on graphene oxide coated qcm", ***Polish Journal of Environmental Studies***, Vol. 31, No. 4, (2022), 1-7. doi: 10.15244/pjoes/147057.
13. Lee, J., Jang, J., Akin, D., Savran, C.A. and Bashir, R., "Real-time detection of airborne viruses on a mass-sensitive device", ***Applied Physics Letters***, Vol. 93, No. 1, (2008), 013901. doi: 10.1063/1.2956679.
14. Morris, D.R., Fatisson, J., Olsson, A.L., Tufenkji, N. and Ferro, A.R., "Real-time monitoring of airborne cat allergen using a qcm-based immunosensor", ***Sensors and Actuators B: Chemical***, Vol. 190, (2014), 851-857. doi: 10.1016/j.snb.2013.09.061.
15. Wang, P., Su, J., Dai, W., Cernigliaro, G. and Sun, H., "Ultrasensitive quartz crystal microbalance enabled by micropillar structure", ***Applied Physics Letters***, Vol. 104, No. 4, (2014), 043504. doi: 10.1063/1.4862258.
16. Zaza, G., Hammou, A., Benchatti, A. and Saiah, H., "Fault detection method on a compressor rotor using the phase variation of the vibration signal", ***International Journal of Engineering***, ***Transactions B: Applications,*** Vol. 30, No. 8, (2017), 1176-1181. doi: 10.5829/ije.2017.30.08b.09.
17. Wang, P., Su, J., Su, C.-F., Dai, W., Cernigliaro, G. and Sun, H., "An ultrasensitive quartz crystal microbalance-micropillars based sensor for humidity detection", ***Journal of Applied Physics***, Vol. 115, No. 22, (2014), 224501. doi: 10.1063/1.4880316.
18. Su, J., Esmaeilzadeh, H., Zhang, F., Yu, Q., Cernigliaro, G., Xu, J. and Sun, H., "An ultrasensitive micropillar-based quartz crystal microbalance device for real-time measurement of protein immobilization and protein-protein interaction", ***Biosensors and Bioelectronics***, Vol. 99, (2018), 325-331. doi: 10.1016/j.bios.2017.07.074.
19. Kashan, M., Kalavally, V., Lee, H. and Ramakrishnan, N., "Resonant characteristics and sensitivity dependency on the contact surface in qcm-micropillar-based system of coupled resonator sensors", ***Journal of Physics D: Applied Physics***, Vol. 49, No. 19, (2016), 195303. doi: 10.1088/0022-3727/49/19/195303.
20. Kashan, M.A.M., Kalavally, V. and Ramakrishnan, N., "Sensing film-coated qcm coupled resonator sensors: Approach, fabrication, and demonstration", ***Sensors and Actuators A: Physical***, Vol. 274, (2018), 64-72. doi: 10.1016/j.sna.2018.03.006.
21. Mulyawati, I.B., Riza, M., Dermawan, H. and Pratiwi, V., "Numerical simulation of embankment settlement in vacuum preloading systems", ***International Journal of Engineering***, ***Transactions A: Basics***, Vol. 36, No. 4, (2023), 817-823. doi: 10.5829/IJE.2023.36.04A.18
22. Thepade, S., Dindorkar, M., Chaudhari, P. and Bang, S., "Enhanced face presentation attack prevention employing feature fusion of pre-trained deep convolutional neural network model and thepade's sorted block truncation coding", ***International Journal of Engineering***, ***Transactions A: Basics***, Vol. 36, No. 4, (2023), 807-816. doi: 10.5829/IJE.2023.36.04A.17
23. Marchione, F., "Shear stress distribution in double-lap adhesive joints reinforced with nylon fabric: Numerical investigation", ***International Journal of Engineering***, ***Transactions A: Basics***, Vol. 36, No. 1, (2023), 35-40. doi: 10.5829/IJE.2023.36.01A.05
24. Abdollahi, S.A., Alizadeh, A.a., Chiniforooshan Esfahani, i., Zarinfar, M. and Pasha, P., "Investigating heat transfer and fluid flow betwixt parallel surfaces under the influence of hybrid nanofluid suction and injection with numerical analytical technique", ***Alexandria Engineering Journal***, Vol. 70, (2023), 423-439. doi: 10.1016/j.aej.2023.02.040.

25. Kashan, M.A.M., Kalavally, V., Mazumdar, P., Lee, H.W. and Ramakrishnan, N., "Qcm coupled resonating systems under vacuum: Sensitivity and characteristics", ***IEEE Sensors Journal***, Vol. 17, No. 16, (2017), 5044-5049. doi: 10.1109/JSEN.2017.2719104.
26. Wang, P., Su, J., Shen, M., Ruths, M. and Sun, H., "Detection of liquid penetration of a micropillar surface using the quartz crystal microbalance", ***Langmuir***, Vol. 33, No. 2, (2017), 638-644. doi: 10.1021/acs.langmuir.6b03640.
27. Esfahani, I.C. and Sun, H., "A droplet-based micropillar-enhanced acoustic wave (μpaw) device for viscosity measurement", ***Sensors and Actuators A: Physical***, Vol. 350, (2023), 114121. doi: 10.1016/j.sna.2022.114121.
28. Xie, X., Xie, J., Luo, W. and Wu, Z., "Electromechanical coupling and frequency characteristics of a quartz crystal resonator covered with micropillars", ***Journal of Vibration and Acoustics***, Vol. 141, No. 4, (2019). doi: 10.1115/1.4042936.
29. Kanazawa, K.K. and Gordon, J.G., "Frequency of a quartz microbalance in contact with liquid", ***Analytical Chemistry***, Vol. 57, No. 8, (1985), 1770-1771. doi: 10.1021/ac00285a062.
30. Mason, W., "Viscosity and shear elasticity measurements of liquids by means of shear vibrating crystals", ***Journal of Colloid Science***, Vol. 3, No. 2, (1948), 147-162. doi: 10.1016/0095-8522(48)90065-8.

Persian Abstract

چکیده

اگرچه تشدید کننده های کریستال کوارتز (QCR) برای تشخیص ذرات و ویروس ها در هوا استفاده شده است، اما از محدودیت های مختلفی مانند حساسیت کم در مقایسه با سایر دستگاه ها رنج می برند. بنابراین، توسعه دستگاه جدیدی با قابلیت دستیابی به حساسیت بالا ضروری است که بتوان از آن برای تشخیص عملی هوابرد استفاده کرد. مطالعه حاضر یک مدل نظری پارامتریک جامع را برای تجزیه و تحلیل پاسخ QCR تقویت‌شده با ستون فوق حساس (QCR-P) برای تشخیص نانوذرات در هوا گزارش می‌کند. مدل الکترومکانیکی شامل یک مدار معادل یکپارچه با ستون های حاوی نانوذرات است. نشان داده شد که ارتفاع ستون و شعاع ذرات نقش مهمی در پاسخ دستگاه‌های QCR-P دارند. این مطالعه نشان داد که انتخاب ارتفاع بهینه ستون می تواند منجر به تغییر فرکانس قابل توجه بسته به شعاع نانوذرات و ارتفاع ستون شود، در حالی که مستقل از چگالی جرم ذرات است. این نتایج بر پتانسیل استفاده از ستون ها برای افزایش قابل ملاحظه حساسیت QCR معمولی تا ۱۴۰ برابر در تشخیص نانوذرات در هوا تأکید می کند. این یافته‌ها را می‌توان برای طراحی ارتفاع ستون‌های بهینه برای دستیابی به حداکثر حساسیت در تشخیص نانوذرات و پروتئین‌ها در هوا مورد استفاده قرار داد، در نتیجه استفاده از تشدید کننده‌های کریستال کوارتز با ستون‌های فوق حساس برای کاربردهای عملی در هوا را ممکن می‌سازد.